J. Biochem. 2011;150(5):563–568 doi:10.1093/jb/mvr096

JB THE JOURNAL OF BIOCHEMISTRY

Structural insight into the stereoselective production of $PGF_{2\alpha}$ by Old Yellow Enzyme from *Trypanosoma cruzi*

Received February 12, 2011; accepted July 13, 2011; published online August 12, 2011

Naoki Okamoto[1], Keishi Yamaguchi[1], Eiichi Mizohata[1], Keiji Tokuoka[1], Nahoko Uchiyama[2], Shigeru Sugiyama[1], Hiroyoshi Matsumura[1], Koji Inaka[3], Yoshihiro Urade[4] and Tsuyoshi Inoue[1,*]

[1]Department of Applied Chemistry, Graduate School of Engineering, Osaka University, 2-1 Yamada-Oka, Suita, Osaka 565-0871; [2]National Institute of Health Sciences (NIHS), Tokyo 158-8501; [3]MARUWA Foods and Biosciences, Inc., 170-1 Tsutsui-cho, Yamatokoriyama, Nara 639-1123; and [4]Department of Molecular Behavior Biology, Osaka Bioscience Institute, Osaka 565-0874, Japan

*Tsuyoshi Inoue, Department of Applied Chemistry, Graduate School of Engineering, Osaka University, 2-1 Yamada-Oka, Suita, Osaka 565-0871, Japan. Fax: +81-6-6879-7409, email: inouet@chem.eng.osaka-u.ac.jp

The atomic coordinates and structure factors of TcOYE/FMN binary complex and TcOYE/FMN/*p*-HBA ternary complex have been deposited with the RCSB Protein Data Bank as 3ATY and 3ATZ, respectively.

Old yellow enzyme (OYE) is an NADPH oxidoreductase capable of reducing a variety of compounds. It contains flavin mononucleotide (FMN) as a prosthetic group. A ternary complex structure of OYE from *Trypanosoma cruzi* (TcOYE) with FMN and one of the substrates, *p*-hydroxybenzaldehyde, shows a striking movement around the active site upon binding of the substrate. From a structural comparison of other OYE complexed with 12-oxophytodienoate, we have constructed a complex structure with another substrate, prostaglandin H_2 (PGH_2), to provide a proposed stereoselective reaction mechanism for the reduction of PGH_2 to prostaglandin $F_{2\alpha}$ by TcOYE.

Keywords: Old yellow enzyme/prostaglandin synthase/ternary complex/X-ray structure.

Abbreviations: FMN, flavin mononucleotide; OPR, 12-oxophytodienoate reductase; OPDA, 12-oxophytodienoate; OYE, old yellow enzyme; PG, prostaglandin; PGFS, prostaglandin $F_2\alpha$ synthase; *p*-HBA, p-hydroxybenzaldehyde; T. cruzi, *Trypanosoma cruzi*; TcOYE, OYE from T. cruzi.

Prostaglandin $F_{2\alpha}$ synthase (PGFS) produces prostaglandin $F_{2\alpha}$ ($PGF_{2\alpha}$) from prostaglandin H_2 (PGH_2), and is found not only in mammals, but also in parasitic protozoa, which cause serious infections (*1*–*6*). In mammals, $PGF_{2\alpha}$ overproduction causes ovarian dysfunction and miscarriage (*7*–*9*). African trypanosomiasis is characterized by miscarriage due to $PGF_{2\alpha}$ overproduction correlated with parasitemia peaks (*7*). Therefore, the study of parasitic PGFS is of interest in order to obtain a better understanding of the pathological roles of $PGF_{2\alpha}$ overproduction and to guide the development of inhibitors. Chagas' disease, caused by (*T. cruzi*), affects more than 20 million people and poses a major public health and economic problem in South America (*10*). Anti-chagasic drugs, such as nifurtimox and 2-nitroimidazole (benznidazole) (*11*–*14*), are available, but the problems of undesirable side effects and parasite resistance of these drugs are still unsolved.

Old yellow enzyme (OYE) containing a vitamin B_2-derived molecule, flavin mononucleotide (FMN), essential for its catalytic reaction (*15*, *16*), was discovered in the 1930s, and has since been identified in yeasts (*17*), plants (*18*) and bacteria (*19*, *20*), but not in animals (Supplementary Fig. 1A and B). *p*-Hydroxybenzaldehyde (*p*-HBA) (*21*) is one of substrates and/or participates in a charge transfer interaction for many OYE family enzymes (Supplementary Fig. 2A). The OYE from *T. cruzi* (TcOYE) was identified and characterized by Kubata *et al*. (*22*), who revealed that TcOYE catalyses $PGF_{2\alpha}$ synthesis as well as the reduction of many kinds of trypanocidal drugs, such as naphthoquinone and nitroheterocyclic compounds (Fig. 1). Therefore, an X-ray crystallographic study of TcOYE with these compounds should provide a structural basis for the development of novel anti-chagasic drugs. Here, we report the ternary complex structure of TcOYE/FMN/*p*-HBA at 2.05 Å resolution. The structure shows the striking movement of a loop covering the active site upon binding of *p*-HBA and reveals the recognition mechanism for a variety of compounds. Furthermore, a proposed PGH_2 binding model leads us to suggest a detailed reaction mechanism from PGH_2 to $PGF_{2\alpha}$ by TcOYE.

Materials and Methods

Enzyme assay

To study *p*-HBA inhibition of TcOYE reductase activity, various concentrations of the inhibitors were pre-incubated with an appropriate amount of NADPH and the reaction was started by the addition of TcOYE. Spectrophotometric assays were performed in a standard reaction mixture (1 ml) containing 100 mM sodium phosphate, pH 7.0, 32 μg/ml TcOYE and 500 μM NADPH. We incubated the mixture at 25°C for 2 min under aerobic conditions before adding the enzyme to initiate the reaction. After the addition of TcOYE, NADPH oxidation was monitored for 1 min by the decrease in absorbance at 340 nm. The reaction rate was determined by calculating initial rates of reaction from the known extinction coefficient of 6,220 $M^{-1}cm^{-1}$ of NADPH.

Preparation of ternary complex crystals of TcOYE/FMN/p-HBA

TcOYE was overexpressed in *Escherichia coli* and purified according to the method as previously reported (*22*, *23*). We first crystallized

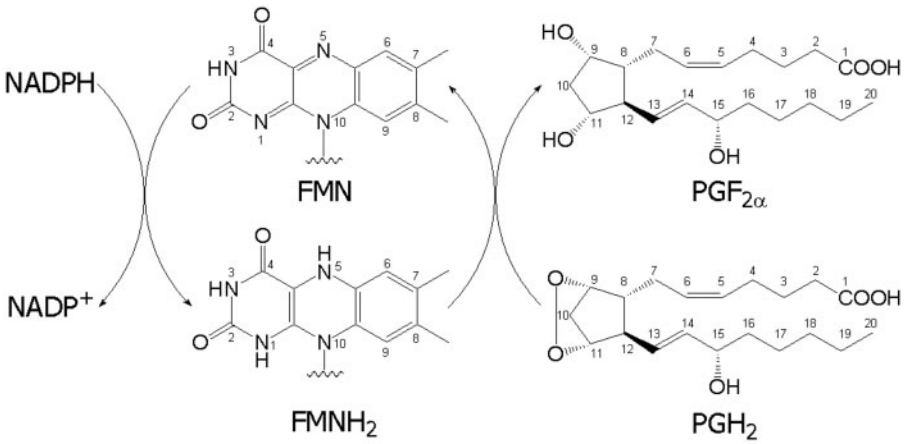

Fig. 1 Reaction scheme of PGH_2 to $PGF_{2\alpha}$ by TcOYE. FMN (cofactor of TcOYE) is reduced to $FMNH_2$ by intravital NADPH, and the product, $PGF_{2\alpha}$, is subsequently generated by $FMNH_2$.

the TcOYE/FMN binary complex, and then the crystals were soaked into the cryo-protectant solution containing 80 mM *p*-HBA and incubated for 2 min. After incubation, the crystals were flash frozen in liquid nitrogen. The X-ray diffraction data were obtained at 2.05 Å resolution at SPring-8 beam-line BL44XU. The diffraction intensity data were processed and scaled using the program HKL2000 (*24*).

Structure determination and refinement

The structure of TcOYE was determined by molecular replacement with the program AMoRe (*25*) using the TcOYE structure previously solved by our group as a search model (*26*). Crystallographic refinement was carried out with the program CNS (*27*). The refinement procedure included simulated annealing, positional refinement, restrained temperature factor refinement and maximum likelihood algorithms as provided by the CNS program. Electron density maps based on the coefficients $2F_o–F_c$ and $F_o–F_c$ were used to build atomic models in Coot (*28*). Water molecules were inserted manually and then checked by inspecting the $F_o–F_c$ map. FMN (cofactor) and *p*-HBA (ligand) were refined using atomic parameters extracted from the HIC-UP server (*29*), and they were inserted into the clearly defined electron density model after some cycles of refinement.

Table I. Data collection and refinement statistics.

	TcOYE/FMN/*p*-HBA
Beam line	SPring-8 BL44XU
Space group	$P2_1$
Cell constants (Å, °)	$a=47.33$, $b=119.59$, $c=111.53$, $\beta=90.35$
Resolution range (Å)	50.0–2.05 (2.12–2.05)[a]
No. of molecules per asymmetric unit	4
V_M (Å^3/dalton)	1.9
V_{solv} (%)	35
No. of measured reflections	297,037
No. of unique reflections	78,333
I/σ (I)	10.2
R_{merge} (%)[b]	9.0 (33.6)[a]
Completeness (%)	100.0 (100.0)[a]
R_{cryst} (%)[c]	18.1
R_{free} (%)[d]	22.9
R.m.s.d.'s	
Bonds (Å)	0.005
Angles (°)	1.3

[a]Values in parentheses are for the highest resolution shell
[b]$R_{merge}=\Sigma|I(k)-I|/\Sigma I(k)$, where $I(k)$ is value of the kth measurement of the intensity of a reflection, I is the mean value of the intensity of that reflection and the summation is over all measurements.
[c]$R_{cryst}=\Sigma||F_o|-|F_c||/\Sigma|F_o|$, calculated from 90% of the data, which were used during the course of the refinement.
[d]$R_{free}=\Sigma||F_o|-|F_c||/\Sigma|F_o|$, calculated from 10% of the data, which were obtained during the course of the refinement.

Results and discussion

Reduction activity of TcOYE for p-HBA as a substrate

p-HBA is one of substrates for enzymes belonging to the OYE family. Therefore, $PGF_{2\alpha}$ synthesis by TcOYE must be competitively inhibited in the presence of *p*-HBA. To gain insight into the binding affinity of *p*-HBA to TcOYE as well as the inhibitory effect on PGH_2 9,11-endoperoxide reductase activity of the enzyme, we investigated the effects of *p*-HBA on NADPH oxidation by TcOYE. *p*-HBA inhibited NADPH oxidation in a dose-dependent manner (Supplementary Fig. 2) and TcOYE exhibited 50% of the control activity in the presence of 57 μM *p*-HBA, indicating that this ligand was an inhibitor for the synthesis of $PGF_{2\alpha}$ also in a dose-dependent manner.

p-HBA binding structure of TcOYE

The three-dimensional structure of the ternary complex of TcOYE/FMN/*p*-HBA was determined by molecular replacement using the native structure (*26*) as the initial model, and refined at 2.05 Å resolution with final R_{cryst}/R_{free} values of 18.1%/22.9% (Table I).

TcOYE, like other members of the OYE family, folds into a $(\alpha/\beta)_8$ barrel in which *p*-HBA is clearly bound at the C-terminal ends of the 8 β-strands (Fig. 2A). The structure comparison between the ternary complex of TcOYE/FMN/*p*-HBA and the binary complex of TcOYE/FMN provides information about the structural changes that occur upon binding of *p*-HBA (Supplementary Fig. 2C). While the r.m.s.d. value for Cα carbon atoms in the whole structure was calculated to be 0.34 Å, the value for Loop 1 from Lys140 to Thr157 was found to be 1.1 Å. The region from Lys140 to Tyr157 in Loop 1 was obviously shifted away from the active site of TcOYE upon binding of *p*-HBA.

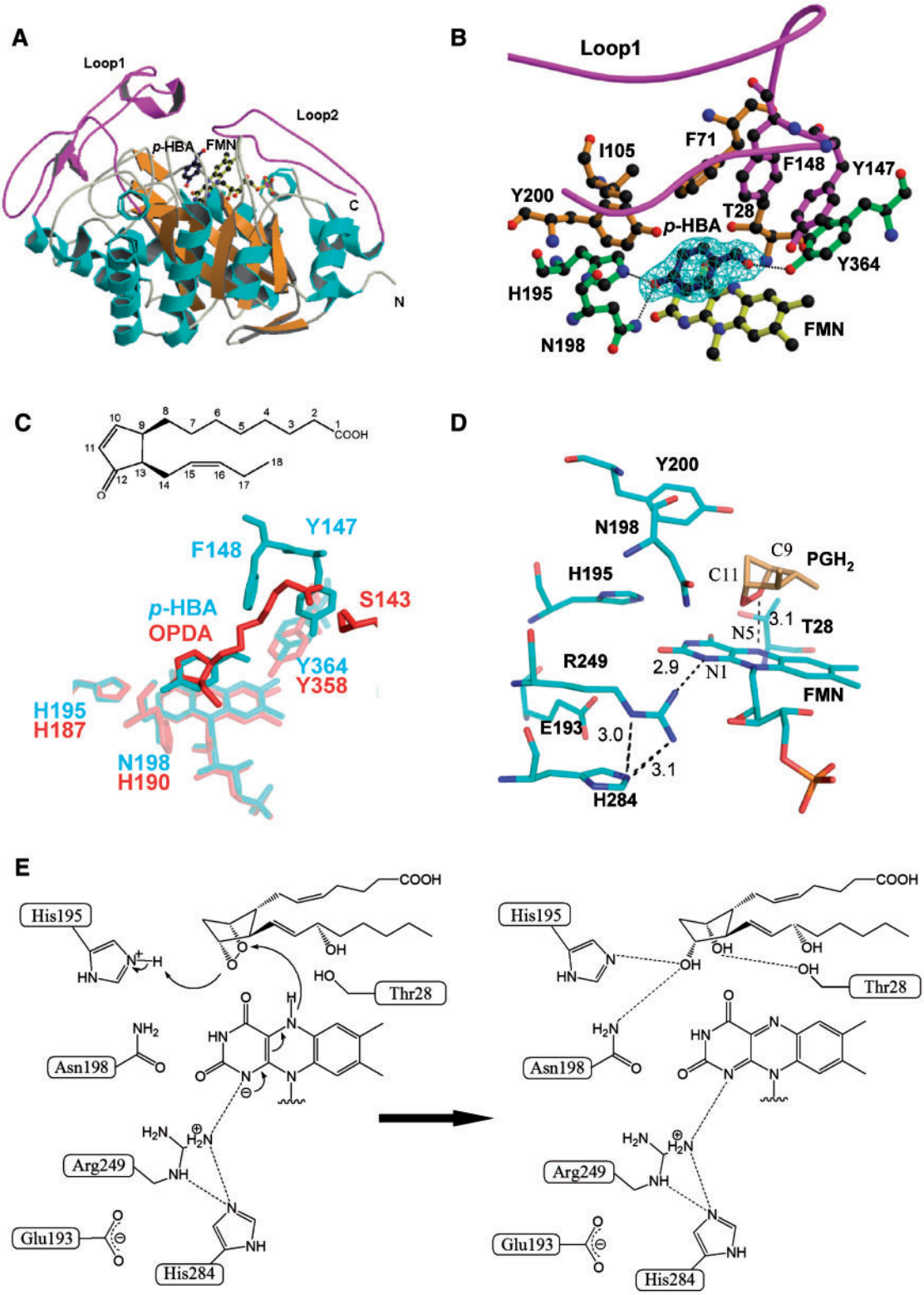

Fig. 2 Recognition of *p*-HBA by TcOYE. (A) Schematic representation of the ternary complex of TcOYE/FMN/*p*-HBA. The α-helices (in cyan) and β-sheets (in orange) are separated by loops (in light yellow). The loops shown in magenta (Loop1 and Loop2) are those related to the substrate recognition of TcOYE. FMN and p-HBA are shown as a ball-and-stick model. (B) A close-up view of the ligand binding site. A *p*-HBA molecule (dark blue) is positioned above the isoalloxazine ring of FMN and forms hydrogen bonds (represented in dashed lines) with 3 residues (green) of TcOYE. The *p*-HBA electron density is calculated at 2.05 Å and contoured at 1.0 σ. Residues shown in orange (highly conserved in OYEs) and magenta (in Loop1 unique to TcOYE) form a hydrophobic pocket surrounding the active site of TcOYE. (C) A close-up view of the active site of TcOYE (cyan) superimposed with that of OPR1 (red) by using the C_α carbon atoms of whole structures. A part of the olefinic side chain of OPDA is disordered in the structure of OPR1; however, the cyclopentane ring of OPDA is superimposed on p-HBA in the structure of TcOYE. Ligands and residues of Loop1 in both enzymes are shown with no transparency. (D) Side view of the proposed structure of TcOYE complexed with PGH_2. (E) Proposed mechanism of PGH_2 reduction by TcOYE. A hydride is expected to be transferred from N5 of FMN to the C9 oxygen of PGH_2, whereas a proton would be donated from His195 to the C11 oxygen of PGH_2. The figures of (A) and (B) were drawn by using the program MOLSCRIPT (*36*) and RASTER3D (*37*), and those of (C) and (D) were created by PyMOL (*38*).

The *p*-HBA molecule is well-defined in the electron density of difference Fourier maps and is placed above the isoalloxazine ring of FMN via a π–π interaction (Fig. 2B). Besides, the ligand is stabilized by three hydrogen bonds: His195 and Asn198 interact with the phenolate oxygen and Tyr364 with the aldehyde carbonyl oxygen of the *p*-HBA molecule. His195 and Tyr364 are almost exclusively conserved among the OYE family. Asn198 is conserved as an asparagine or histidine where both N_δ atoms are involved with the binding to FMN (residues represented by *green stars* in Supplementary Fig. 1).

Like other OYE families, the active site of TcOYE is surrounded with hydrophobic residues (*30*, *31*), and the aromatic ring of *p*-HBA is stabilized in this hydrophobic pocket. Most residues forming the pocket are present in previously solved OYE members: Thr28 and Tyr200 are conserved also in other OYE members; however, Phe71 and Ile105 are conserved as tyrosine and tryptophan, respectively. It is notable that Tyr147 and Phe148 are characteristic of TcOYE.

Structural comparison of TcOYE with OPR1

12-Oxophytodienoate reductase (OPR) from *Lycopersicon esculentum* (tomato), an OYE homologue containing a cofactor of FMN, catalyses the NADPH-dependent reduction of the cyclopentenone, 12-oxophytodienoate (OPDA) (*32*, *33*), whose skeleton is similar to PGH_2, another substrate of TcOYE (*30*) (Fig. 2C & Supplementary Fig. 3A). OPR1 from *Lycopersicon esculentum* is one of the isoforms of OPR, and shares 36% sequence identity with TcOYE (Supplementary Fig. 1). Even with the low sequence identity, the complex structure of TcOYE/FMN/*p*-HBA was superimposed on that of OPR1/FMN/OPDA with a r.m.s.d. value of 1.1 Å for the Cα carbon atoms (Supplementary Fig. 3B). However, the structural difference between TcOYE and OPR1 was striking at Loop1.

As for the binding of OPDA, the carbonyl oxygen at C12 is hydrogen-bonded to His187(Nε) and His190(Nδ), and the carboxyl group of the α-chain interacts with Ser143(OH) in Loop1. The phenolate oxygen of *p*-HBA is hydrogen bonded to His195(Nε) and Asn198(Nδ) that are conserved as His187 and His190 in OPR1, respectively. Besides, Tyr364, which is hydrogen-bonded to the aldehyde carbonyl oxygen of *p*-HBA, is conserved as Tyr358 in OPR1 (Fig. 2C). In OPR1, Ser143 interacts with the carboxyl group of OPDA, but the corresponding residue is not conserved in Loop1 of TcOYE. Ser143 in OPR1 corresponds to Tyr147 or Phe148 in Loop1 of TcOYE (Supplementary Fig. 1A); however, both of the residues are quite close to the α-chain of OPDA (Fig. 2C). If an OPDA molecule were inserted into the active site of TcOYE, the α-chain of OPDA in its conformation in OPR1 would conflict with Tyr147 and Phe148 in Loop1 of TcOYE. Because the molecular formula of OPDA is quite similar with that of PGH_2, if a PGH_2 molecule binds to the active site of TcOYE as the substrate, a larger structural movement of Loop1 would also be expected to occur to avoid the steric hindrances contributed by Tyr147 and Phe148 and to bring together the α-chain of the substrate with some residue instead of Ser143 in OPR1. Notably, not only in OPR1 but also in the other solved OYEs, Loop1 was involved in binding to various ligands (*31*, *34*); therefore, TcOYE might have evolved to recognize a PGH_2 molecule as its substrate by acquiring the uniqueness and flexibility contained in the structure of Loop1.

PGH_2 binding model of TcOYE and proposed reaction mechanism as PGFS

The initial three-dimensional coordinate and its molecular topology of the substrate PGH_2 were generated by using the HIC-Up server ('Hetero-compound Information Centre, Uppsala, at URL http://alpha2.bmc.uu.se/hicup/). Because the structure formula of PGH_2 is similar with that of OPDA, we then modelled the PGH_2 molecule manually based on the coordinates of the OPR1/FMN/OPDA complex. The cyclopentane ring and the α-chain of PGH_2 were first superimposed on those of OPDA, and a binding model of PGH_2 was then constructed with energy minimization by using the conformational database potential method implemented in the refinement program CNS (*27*) (Fig. 2D). In CNS, the Engh and Huber force field (as described in chapter 18.3 of volume F of International Table for Crystallography, pp. 382–392, 2001) is used. As for the FMN molecule, we examined the energy minimization with both the reduced form of $FMNH^-$ and $FMNH_2$, but the relative positions of the cyclopentane ring of PGH_2 and its surroundings were not strikingly changed. Finally, the surface representation showed that PGH_2 could be bound into the active site which is surrounded by many hydrophobic residues (Supplementary Fig. 3C). The hydrophobic pocket probably stabilizes the alkyl chains of PGH_2 while the α-chain of PGH_2 was located in the pocket formed by Tyr363, Tyr364 and Pro360 in the current model.

TcOYE catalyses one- or two-electron reduction of various substrates (*22*). Therefore, two possible mechanisms can be envisaged for the reduction of the substrate PGH_2 by a reduced flavin in TcOYE. One mechanism is the one-electron reduction including sequential electron and proton transfer. The other mechanism is the two electron reduction including hydride transfer. In case of the former, N5 or N1 of FMN could be possible as the proton or electron donor for the C9 or C11 oxygen of PGH_2, respectively, because, in Fig. 2D, the distances between N5 and the C9 oxygen and between N1 and the C11 oxygen are calculated to be 3.1 and 3.3 Å, respectively. If the reaction of PGH_2 to $PGF_{2\alpha}$ in TcOYE occurs by two-electron reduction, it appears that a hydride transfers from N5 of FMN to the C9 oxygen of PGH_2 (distance 3.1 Å), and the proton donor for the C11 oxygen is thought to be Nε of His195 (Fig. 2D). Indeed the C11 oxygen of PGH_2 is located at 5.5 Å from Nε of His195 and at 3.5 Å from Nε of Asn198 in this model, but the C11 oxygen would be accessible to both His195 and Asn198 upon cleaving the peroxide after the acceptance of a hydride at the C9 oxygen of PGH_2. The C9 oxygen after the reduction also could hydrogen bond to the

OH atom of Thr28 (positioned at 4.1 Å from C9 oxygen in Fig. 2D). In this reaction, N_δ of His284 is located at 3.3 Å from Nε of Arg249, and at 3.4 Å from Oε of Glu193. It is likely that a triad of Glu193–His284–Arg249 is stabilized by these interactions. All residues in Fig. 2D are strongly conserved in OYE members and play an important role in the reduction of PGH_2 by TcOYE (Fig. 2D).

As for many other OYE families, tyrosine (corresponding to Tyr200 in TcOYE) is utilized as a proton source for substrates (*35*). In TcOYE, however, Tyr200 cannot provide a proton to PGH_2 because the C9 and C11 oxygen atoms need to accept a hydride or proton from the same direction to maintain the stereospecificity of the biosynthesis of $PGF_{2\alpha}$ by TcOYE. Hence, it is reasonable that proton transfer from His195 under the cyclopentane ring of PGH_2, instead of Tyr200, would occur to achieve the stereoselective production of $PGF_{2\alpha}$ (Fig. 2D and E).

We believe that the structural analysis of the ternary complex of TcOYE/FMN/p-HBA as it primarily relates to substrate binding of PGH_2 may lead to the development of heroic anti-chagasic drugs.

Supplementary Data

Supplementary Data are available at *JB* online.

Acknowledgements

The authors express their appreciation to Professor B. K. Kubata, Biosciences Eastern and Central Africa, and Dr Z. Kabututu, Osaka Bioscience Institute, for their early support of protein expression. The authors are grateful to M. Yoshimura, M. Yamashita, E. Yamashita and A. Nakagawa for their kind support during data collection at SPring-8 beamline 44XU.

Funding

Grants-in-Aid for Scientific Research (No. 22550152) from the Ministry of Education, Culture, Sports, Science and Technology of Japan and the PRESTO project, Japan Science and Technology Agency, the National Project on Protein Structural and Functional Analyses, Japan (to T.I.); High-quality Protein Crystal Growth Experiment on JEM promoted by JAXA and Osaka City (to Y.U.).

Conflict of interest

None declared.

References

1. Kilunga Kubata, B., Eguchi, N., Urade, Y., Yamashita, K., Mitamura, T., Tai, K., Hayaishi, O., and Horii, T. (1998) Plasmodium falciparum produces prostaglandins that are pyrogenic, somnogenic, and immunosuppressive substances in humans. *J. Exp. Med.* **188**, 1197–1202
2. Kubata, B.K., Duszenko, M., Kabututu, Z., Rawer, M., Szallies, A., Fujimori, K., Inui, T., Nozaki, T., Yamashita, K., Horii, T., Urade, Y., and Hayaishi, O. (2000) Identification of a novel prostaglandin $F_{2\alpha}$ synthase in Trypanosoma brucei. *J. Exp. Med.* **192**, 1327–1338
3. Okano, Y., Inoue, T., Kubata, B.K., Kabututu, Z., Urade, Y., Matsumura, H., and Kai, Y. (2002) Crystallization and preliminary X-ray crystallographic studies of Trypanosoma brucei prostaglandin $F_{2\alpha}$ synthase. *J. Biochem.* **132**, 859–861
4. Kilunga Kubata, B., Inoue, T., Okano, Y., Kabututu, Z., Martin, S.K., Lazarus, M., Duszenko, M., Sumii, Y., Kusakari, Y., Matsumura, H., Kai, Y., Sugiyama, S., Inaka, K., Inui, T., and Urade, Y. (2005) Structural and mutational analysis of Trypanosoma brucei prostaglandin H_2 reductase provides insight into the catalytic mechanism of aldo-ketoreductases. *J. Biol. Chem.* **280**, 26371–26382
5. Kabututu, Z., Martin, S.K., Nozaki, T., Kawazu, S., Okada, T., Munday, C.J., Duszenko, M., Lazarus, M., Thuita, L.W., Urade, Y., and Kubata, B.K. (2002) Prostaglandin production from arachidonic acid and evidence for a 9,11-endoperoxide prostaglandin H_2 reductase in Leishmania. *Int. J. Parasitol.* **32**, 1693–1700
6. Kabututu, Z., Martin, S.K., Nozaki, T., Kawazu, S., Okada, T., Munday, C.J., Duszenko, M., Lazarus, M., Thuita, L.W., Urade, Y., and Kubata, B.K. (2003) Prostaglandin production from arachidonic acid and evidence for a 9,11-endoperoxide prostaglandin H_2 reductase in Leishmania. *Int. J. Parasitol.* **33**, 221–228
7. Mutayoba, B.M., Meyer, H.H.D., Osaso, J., and Gombe, S. (1989) Trypsnosome-induced increase in prostaglandin $F_{2\alpha}$ and its relationship with corpus luteum function in the goat. *Theriogenology* **32**, 545–555
8. Davies, P., Bailey, P.J., Goldenberg, M.M., and Ford-Hutchinson, A.W. (1984) The role of arachidonic acid oxygenation products in pain and inflammation. *Annu. Rev. Immunol.* **2**, 335–357
9. Dubois, R.N., Abramson, S.B., Crofford, L., Gupta, R.A., Simon, L.S., Van De Putte, L.B., and Lipsky, P.E. (1998) Cyclooxygenase in biology and disease. *Faseb J.* **12**, 1063–1073
10. World Health Organization. (1990) Chagas disease: frequency and geographycal distribution. *Wkly. Epidemiol. Rec.* **65**, 257–261
11. Aldunate, J. and Morello, A. (1993) *Free radicals in the mode of action of antiparasitic drugs*, Harwood Academic Publisher, GmbH, Chur, Switzerland
12. Henderson, G.B., Ulrich, P., Fairlamb, A.H., Rosenberg, I., Pereira, M., Sela, M., and Cerami, A. (1988) "Subversive" substrates for the enzyme trypanothione disulfide reductase: alternative approach to chemotherapy of Chagas disease. *Proc. Natl. Acad. Sci. U S A* **85**, 5374–5378
13. Docampo, R. and Moreno, S.N. (1986) Free radical metabolism of antiparasitic agents. *Fed. Proc.* **45**, 2471–2476
14. Docampo, R. (1990) Sensitivity of parasites to free radical damage by antiparasitic drugs. *Chem. Biol. Interact.* **73**, 1–27
15. Warburg, O. and Christian, W. (1933) Über das gelbe Ferment und seine Wirkungen. *Biochem. Z.* **266**, 377–411
16. Schopfer, L.M. and Massey, V. (1991) *Old yellow enzyme*, CRC Press, Boston
17. Matthews, R.G., Massey, V., and Sweeley, C.C. (1975) Identification of p-hydroxybenzaldehyde as the ligand in the green form of old yellow enzyme. *J. Biol. Chem.* **250**, 9294–9298
18. Schaller, F. and Weiler, E.W. (1997) Molecular cloning and characterization of 12-oxophytodienoate reductase, an enzyme of the octadecanoid signaling pathway from Arabidopsis thaliana. Structural and functional relationship to yeast old yellow enzyme. *J. Biol. Chem.* **272**, 28066–28072

19. French, C.E., Nicklin, S., and Bruce, N.C. (1996) Sequence and properties of pentaerythritol tetranitrate reductase from Enterobacter cloacae PB2. *J. Bacteriol.* **178**, 6623–6627
20. Blehert, D.S., Fox, B.G., and Chambliss, G.H. (1999) Cloning and sequence analysis of two Pseudomonas flavoprotein xenobiotic reductases. *J. Bacteriol.* **181**, 6254–6263
21. Abramovitz, A.S. and Massey, V. (1976) Interaction of phenols with old yellow enzyme. Physical evidence for charge-transfer complexes. *J. Biol. Chem.* **251**, 5327–5336
22. Kubata, B.K., Kabututu, Z., Nozaki, T., Munday, C.J., Fukuzumi, S., Ohkubo, K., Lazarus, M., Maruyama, T., Martin, S.K., Duszenko, M., and Urade, Y. (2002) A key role for old yellow enzyme in the metabolism of drugs by Trypanosoma cruzi. *J. Exp. Med.* **196**, 1241–1251
23. Sugiyama, S., Tokuoka, K., Uchiyama, N., Okamoto, N., Okano, Y., Matsumura, H., Inaka, K., Urade, Y., and Inoue, T. (2007) Preparation, crystallization and preliminary crystallographic analysis of old yellow enzyme from Trypanosoma cruzi. *Acta Crystallogr. Sect. F Struct. Biol. Cryst. Commun.* **63**, 896–898
24. Otwinowski, Z. and Minor, W. (1997) Processing of X-ray diffraction data collected in oscillation mode. *Methods Enzymol.* **276**, 307–326
25. Navaza, J. (2001) Implementation of molecular replacement in AMoRe. *Acta Crystallogr. D Biol. Crystallogr.* **57**, 1367–1372
26. Yamaguchi, K., Okamoto, N., Tokuoka, K., Sugiyama, S., Uchiyama, N., Matsumura, H., Inaka, K., Urade, Y., and Inoue, T. (2011) Structure of the inhibitor complex of old yellow enzyme from Trypanosoma cruzi. *J. Synchrotron Radiat.* **18**, 66–69
27. Brunger, A.T., Adams, P.D., Clore, G.M., DeLano, W.L., Gros, P., Grosse-Kunstleve, R.W., Jiang, J.S., Kuszewski, J., Nilges, M., Pannu, N.S., Read, R.J., Rice, L.M., Simonson, T., and Warren, G.L. (1998) Crystallography & NMR system: A new software suite for macromolecular structure determination. *Acta Crystallogr. D Biol. Crystallogr.* **54**, 905–921
28. Emsley, P. and Cowtan, K. (2004) Coot: model-building tools for molecular graphics. *Acta Crystallogr. D Biol. Crystallogr.* **60**, 2126–2132
29. Kleywegt, G.J. and Jones, T.A. (1998) Databases in protein crystallography. *Acta Crystallogr. D Biol. Crystallogr.* **54**, 1119–1131
30. Breithaupt, C., Strassner, J., Breitinger, U., Huber, R., Macheroux, P., Schaller, A., and Clausen, T. (2001) X-ray structure of 12-oxophytodienoate reductase 1 provides structural insight into substrate binding and specificity within the family of OYE. *Structure* **9**, 419–429
31. van den Hemel, D., Brige, A., Savvides, S.N., and Van Beeumen, J. (2006) Ligand-induced conformational changes in the capping subdomain of a bacterial old yellow enzyme homologue and conserved sequence fingerprints provide new insights into substrate binding. *J. Biol. Chem.* **281**, 28152–28161
32. Vick, B.A. and Zimmerman, D.C. (1986) Characterization of 12-oxo-phytodienoic acid reductase in corn: the jasmonic acid pathway. *Plant Physiol.* **80**, 202–205
33. Schaller, F. (2001) Enzymes of the biosynthesis of octadecanoid-derived signalling molecules. *J. Exp. Bot.* **52**, 11–23
34. Barna, T.M., Khan, H., Bruce, N.C., Barsukov, I., Scrutton, N.S., and Moody, P.C. (2001) Crystal structure of pentaerythritol tetranitrate reductase: ''flipped'' binding geometries for steroid substrates in different redox states of the enzyme. *J. Mol. Biol.* **310**, 433–447
35. Kohli, R.M. and Massey, V. (1998) The oxidative half-reaction of Old Yellow Enzyme. The role of tyrosine 196. *J. Biol. Chem.* **273**, 32763–32770
36. Kraulis, P.J. (1991) MOLSCRIPT: a program to produce both detailed and schematic plots of protein structures. *J. Appl. Crystallogr.* **277**, 505–524
37. Merritt, E.A. and Murphy, M.E. (1994) Raster3D Version 2.0. A program for photorealistic molecular graphics. *Acta Crystallogr. D Biol. Crystallogr.* **50**, 869–873
38. DeLano, W.L. (2005) The case for open-source software in drug discovery. *Drug Discov. Today* **10**, 213–217